

See discussions, stats, and author profiles for this publication at: <https://www.researchgate.net/publication/263958227>

Mercury Emissions and Removal by Ash in Coal-Fired Oxy-fuel Combustion

ARTICLE *in* ENERGY & FUELS · NOVEMBER 2013

Impact Factor: 2.79 · DOI: 10.1021/ef4014604

CITATIONS

15

READS

50

8 AUTHORS, INCLUDING:



[Lawrence Phoa Belo](#)

De La Salle University

18 PUBLICATIONS 40 CITATIONS

[SEE PROFILE](#)



[Kalpit Shah](#)

University of Newcastle

39 PUBLICATIONS 225 CITATIONS

[SEE PROFILE](#)



[Rohan Stanger](#)

University of Newcastle

35 PUBLICATIONS 257 CITATIONS

[SEE PROFILE](#)



[T. F. Wall](#)

University of Newcastle

191 PUBLICATIONS 5,249 CITATIONS

[SEE PROFILE](#)

Mercury Emissions and Removal by Ash in Coal-Fired Oxy-fuel Combustion

Reinhold Spörl,^{*,†} Lawrence Belo,[‡] Kalpit Shah,[‡] Rohan Stanger,[‡] Roman Giniyatullin,[†] Jörg Maier,[†] Terry Wall,[‡] and Günter Scheffknecht[†]

[†]Institute of Combustion and Power Plant Technology (IFK), University of Stuttgart, 70569 Stuttgart, Germany

[‡]Chemical Engineering, University of Newcastle, Callaghan, New South Wales 2308, Australia

ABSTRACT: This paper presents results of experiments performed at a 20 kW once-through combustion rig of the Institute of Combustion and Power Plant Technology (IFK) of the University of Stuttgart. A methodology to investigate oxy-fuel process configurations was used in which impurities were injected to the oxidant gas of the once-through reactor to simulate different extents of oxy-fuel recycle gas treatment. Three Australian coals, which had previously been tested in the Aioi furnace of IHI in Japan, were used in the experiments. A comprehensive set of total (Hg^{tot}), elemental (Hg^0), and oxidized (Hg^{2+}) mercury concentrations was measured for various air and oxy-fuel combustion conditions. These data enable an evaluation of process parameters that influence the Hg emissions of an oxy-fuel combustion process. A theoretical mass balance between Hg fed to the process (fuel and Hg^0 injection) and Hg measured before the filter matched well, indicating that no mercury was captured by fly ash at high temperatures. The capture of Hg^0 and oxidized Hg^{2+} by ash in a baghouse filter has been determined for all experiments. Measured Hg concentrations show an increase when switching from air to oxy-fuel operation for all investigated coals and oxy-fuel settings, even when no additional Hg^0 is injected to the oxidant gas. Moreover, the $\text{Hg}^{2+}/\text{Hg}^{\text{tot}}$ ratios in the flue gas are higher during oxy-fuel combustion. The Hg capture by ash in the baghouse filter has been found to reduce the Hg emissions considerably. Reduction rates in a range between 18 and 51% for air and between 11 and 29% for oxy-fuel combustion were observed.

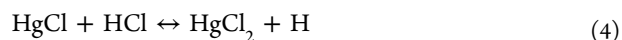
1. INTRODUCTION AND BACKGROUND

1.1. Oxy-fuel Combustion. With a growing awareness on the increased greenhouse gas emissions and their contribution to climate change, CO_2 capture and storage (CCS) and CO_2 capture and utilization (CCU, e.g., in enhanced oil recovery) technologies for coal-fired power generation were developed to concentrate CO_2 for processing and sequestration/utilization. Oxy-fuel combustion is one of the CCS/CCU technologies. In oxy-fuel operation, coal is burned with a mixture of oxygen and recirculated flue gas, instead of air. The mixing of O_2 with recirculated flue gas is, among other issues, necessary to lower the temperature in the furnace, which otherwise would exceed the limits of construction materials of the boiler.¹ Because of the lack of flue gas dilution by airborne N_2 , the concentrations of oxy-fuel flue gas components, such as CO_2 , SO_2 , and H_2O , generally increase considerably by a factor of around 4.^{2,3} NO_x formation is altered, being affected by O_2 injection conditions, burner configurations, and airborne N_2 exclusion from the combustion.⁴ Moreover, higher Hg concentrations in the flue gas during oxy-fuel combustion are expected than in conventional air firing. The higher Hg concentrations have potential implications on environmental pollution as well as corrosion of Al alloys by Hg, which can be particularly problematic in the CO_2 processing unit of an oxy-fuel plant, where Al alloys are applied, e.g., for heat exchangers.⁵

Various oxy-fuel process configurations (wet/dry recycle and environmental control units) as well as process conditions (recycle rate, residence time, and thermal profile) are possible and have a significant impact on the concentration and reactions of impurities, such as NO_x , SO_x , and Hg.^{6,7} For

safety and corrosion issues, these impurities must be controlled and the choice of control units will ultimately affect plant cost and waste streams. The performed experiments show how different fuels and different process configurations impact the Hg^0 and Hg^{2+} concentrations in the flue gas and the Hg removal in a baghouse filter.

1.2. Hg^0 and Hg^{2+} Generation and Capture. Mercury occurs in coals mostly associated with sulfur compounds (e.g., FeS_2) or organic fractions.^{8–11} During combustion, the Hg in the fuel is completely evaporated and converted to its elemental vapor form Hg^0 ,¹² reaching Hg concentrations in a range of 1–20 $\mu\text{g}/\text{m}^3$ in air-fired systems.¹³ During cooling of the flue gases, the interactions with other flue gas compounds cause Hg^0 to become homogeneously oxidized to Hg^{2+} via the following dominant pathway:^{9,12–15}



Special Issue: 4th (2013) Sino-Australian Symposium on Advanced Coal and Biomass Utilisation Technologies

Received: July 29, 2013

Revised: October 11, 2013

Published: October 16, 2013



The direct reaction of Hg with Cl_2 (reaction 2) is much slower than the reaction with Cl (reaction 1) but may be important in environments with depletion of Cl.¹⁶ The direct Hg oxidation reaction with HCl is considered to be of limited importance, because of its slow kinetics,^{9,17} while for the secondary reaction with HgCl (reaction 4), HCl may be more important, as is Cl_2 .¹² Because the Hg oxidation is highly dependent upon the availability of Cl radicals, it may be promoted at higher temperatures under which these radicals are more abundantly available.¹² Higher Cl contents in the fuel can lead to higher Hg oxidation.⁹ Hg oxidation can also occur via heterogeneous reactions, e.g., on fly ash (catalytically active unburned carbon and Fe_2O_3 ^{9,12,18}), injected activated carbon,^{9,14} or selective catalytic reduction (SCR) catalysts.^{8,9,11,14,19} The importance of the heterogeneous Hg oxidation however is varying for different plant layouts, plant loads, and fuels (e.g., Cl and S contents),^{20–22} and some of the observations made in bench scale, such as the catalysis of the Hg oxidation by Fe_2O_3 , could not be reproduced in technical- and industrial-scale facilities.²¹ The $\text{Hg}^0/\text{Hg}^{2+}$ conversion in coal-fired systems, such as power plants, is not complete but kinetically limited^{9,11} and depends upon the availability of Cl (and Br) and catalytically active materials. $\text{Hg}^0/\text{Hg}^{2+}$ conversion also depends upon factors, such as combustion conditions (e.g., combustion stoichiometry)¹² and temperature profile/quench rate of the flue gas (e.g., plant load), which also influences the availability of Cl radicals.^{12,23} A similar but more efficient reaction pathway as with Cl is possible with Br, if a sufficient amount of Br is present in the flue gas¹⁷ (e.g., via CaBr_2 addition to the combustion²⁴). The thermodynamic equilibrium of the Hg oxidation by Cl in flue gases, which depends upon the HCl concentration, predicts that the oxidation of Hg^0 starts around 600–900 °C and completes as it cools to approximately 450–620 °C for HCl concentrations of 50–3000 ppm.¹⁵ Flue gas components, such as H_2O , NO_x , and SO_2 , can influence the oxidation of Hg in the gas phase: H_2O may decrease Hg oxidation by inhibiting the decomposition of HCl to form Cl radicals.¹⁷ Because of the large amount of available H_2O compared to small amounts of Cl in coal combustion systems, the effect of H_2O variation (at high H_2O levels) may be of limited importance in coal combustion. Niksa et al.¹⁷ found in simulations that NO may either increase or suppress Hg oxidation, depending upon the NO concentration level. This effect however may be unimportant in power plants that have higher NO levels, at which the sensitivity of the Hg oxidation upon increasing NO levels was less pronounced.¹⁷ Combustion experiments testing three coals with up to 190 ppm NO_2 injection (at NO_x levels of 1400–1500 ppm) by Galbreath et al.²⁵ showed no significant impact of NO_2 on Hg oxidation. In pulverized coal-fired processes, NO_x is primarily emitted as NO,²⁶ which leads generally to low NO_2 concentrations. However, high NO_2 levels could lead to increased SO_3 concentrations by catalyzing the oxidation of SO_2 to SO_3 in the low temperature region of a coal-fired plant²⁷ and may impact Hg oxidation and capture via the component SO_3 . SO_2 and SO_3 in the flue gas may influence the availability of Cl radicals and reduce the catalytic activity of fly ash for the Hg oxidation,^{9,10} so that high S coals show low Hg oxidation, even if the coals are high in Cl. However, according to Kellie et al.,²⁸ SO_2 may also encourage Hg oxidation. High Ca contents of the

ash may reduce the availability of Cl in the gas phase and therefore Hg oxidation.²⁹

Heterogeneous Hg oxidation can occur on entrained fly ash as well as ash deposited on filters.^{10,30,31} With Cl available, surface carbon can be chlorinated, adsorb, and finally oxidize and chemisorb Hg by a mechanism proposed by Gale et al.³² Ashes with high unburned carbon (UBC) have generally higher Hg removal efficiencies.^{11,12,18,32–34} Hg removal by the ash in filters decreases with increasing temperatures,^{11,19,35} which can be explained by the complex sequence of sorption processes and reactions on the surface, with different temperature-dependent rate constants.^{32,33} Direct capture of Hg^0 on fly ash is believed to be of minor importance, while the sorption of gas-phase Hg^{2+} or Hg^0 with subsequent oxidation to Hg^{2+} and capture of the oxidized Hg on the surface seems to be more important for the removal of Hg on fly ashes in filters.³¹ If only little carbon or other sorption sites are available in the ash or available sorption sites are consumed by Hg^{2+} or sulfur species, the chlorinated Hg generated on the ash may desorb and lead to an overall oxidation of gas-phase Hg without significant Hg removal.^{9,31,32} The Hg oxidation on fly ash can be promoted by acid gases, such as HCl, SO_2 , or H_2SO_4 ,^{12,33,36} while increased $\text{SO}_3/\text{H}_2\text{SO}_4$ are reported to decrease the potential for sorption of Hg^{2+} , because both species adsorb on the same sorption sites on carbon surfaces.^{9,11,14,37,38} Ca in the ash synergistically with carbon can affect the Hg capture beneficially, by offering sorption sites for chlorinated Hg.³² Moreover, the poisoning effect of $\text{SO}_3/\text{H}_2\text{SO}_4$ on Hg sorption may be beneficially affected by Ca or alkalis in the ash that can absorb $\text{SO}_3/\text{H}_2\text{SO}_4$.^{14,32,38} Besides the content of UBC in the ash, its structure and surface area are of major importance for Hg capture.^{12,18} Particularly, low-rank-coal-derived carbons are found to be superior to those from bituminous coals in their Hg capture behavior.³³ High filter ash loadings may improve the Hg capture on filters.²⁵ Besides UBC, Hg species may also be adsorbed on inorganic fly ash components or purposely added mineral-based sorbents.¹²

Removal efficiencies of Hg in flue gas cleaning equipment are affected by factors such as Cl and S contents of coal, composition of ash (e.g., UBC), degree of Hg oxidation at the cleaning equipment inlet, and type and operation mode of the applied flue gas cleaning equipment.^{11,19,30} Generally, low-rank coals show lower Hg removal efficiencies than higher rank coals,^{11,39} which is believed to be connected to the lower UBC generated during combustion of those fuels¹¹ and their Cl contents that are often lower than in high-rank coals. As shown by Pavlish et al.,³⁹ the scatter of reported Hg removal efficiencies in different flue gas cleaning unit operations is high but significantly differing for the different coal types. For example, baghouse filter systems in bituminous-coal-fired systems typically can be expected to remove between 40 and 90% of the Hg in the flue gas, while for sub-bituminous-coal-fired systems, this is 20–75% and, in lignite-fired systems, only 0–10%.³⁹ Besides in baghouse filter systems, Hg removal can take place in electrostatic precipitators (ESPs) and flue gas desulfurization (FGD) and can be promoted by activated carbon injection.^{19,39}

Overall, the most important factors influencing the concentration levels, speciation, and removal of Hg from flue gas are the Hg content of coal, Cl (and Br) content of coal, combustion conditions in the furnace, SO_x concentrations and speciation, fly ash properties (UBC, Ca, and catalytically active compounds), residence time and temperature profile of the flue

gas, and emission control devices (e.g., filters, ESP, SCR, and FGD).

For oxy-fuel combustion, only limited information on the Hg emission behavior is available. The impact of the change from a N_2 to a CO_2 atmosphere was shown to have no considerable impact on equilibrium concentrations of Hg^0 and $HgCl_2$.⁴⁰ Comparative lab-scale coal combustion experiments in N_2/O_2 and CO_2/O_2 atmospheres⁴¹ and pilot-scale tests in air and oxy-fuel combustion mode⁷ revealed no differences in the behavior of the Hg oxidation in both atmospheres.⁴¹ In other pilot-scale tests, some alteration of the Hg oxidation when comparing air and oxy-fuel operation was observed, but trends were not clear for different coals.³⁵ The Hg speciation and capture in oxy-fuel systems can be impacted by a considerable increase of the H_2O , HCl, SO_x , and Hg concentrations in the flue gas, because of the exclusion of diluting N_2 from the combustion and a change in the flue gas NO_x concentrations.³⁹ Accordingly, oxy-fuel combustion in pilot scale showed a doubling⁷ or tripling³⁵ of Hg concentrations in the flue gas compared to air firing. Changes in the HCl, SO_x , and Hg concentrations can potentially improve Hg oxidation but may also decrease Hg capture and depend upon the kind and extent of recycle gas cleaning in an oxy-fuel system. A system with full cleaning of the recycled flue gas should exhibit only minor differences to an air system, while in an uncleaned oxy-fuel recycle system, considerable differences in the Hg oxidation and capture are possible.³⁹ Changes in the ash loadings in oxy-fuel combustion with increased oxidant O_2 and changes in the temperature profile in the oxy-fuel combustion process because of changed thermal properties of the oxy-fuel flue gas can also affect Hg oxidation and capture.³⁹ Moreover, the increased residence time of flue gases that are partially recycled and therefore pass flue gas cleaning equipment several times can improve the Hg emission behavior.

This work was conducted to address some of the above-mentioned uncertainties in the literature, by quantifying the change in speciation and extent of capture of gaseous Hg by ash when switching from air to oxy-fuel firing. Injection of impurities to the oxidant gas was used to simulate recycle concentrations of impurities without adversely affecting the reactor configuration. Using this method, it was possible to provide gas concentrations comparable to both fully cleaned "cold" recycle conditions and "hot recycle" impurity levels associated with limited (that is, practical) flue gas cleaning.

2. EXPERIMENTAL SECTION

2.1. Experimental Rig. The experiments were performed at a 20 kW_{th} electrically heated once-through combustion rig (Figure 1) of the Institute of Combustion and Power Plant Technology (IFK), University of Stuttgart, Stuttgart, Germany. The electrically heated furnace (length, 2.5 m; diameter, 0.2 m) was operated at a wall temperature of 1350 °C, with a constant gas product rate of about 11.5 m^3 [standard temperature and pressure (STP)]/h to maintain comparable gas residence times in the system for all experimental settings. After the furnace (furnace residence time of about 4 s), approximately 9–10 m^3 (STP)/h of the generated flue gases were drawn through an electrically heated flue gas duct (remaining gas going to an exhaust), in which the gas temperature drops from approximately 700 to 200 °C in about 4 s. Flue gas enters the heated baghouse filter at gas temperatures of approximately 225 °C (± 30 K) and exits at about 195 °C (± 15 K).

In the air-firing mode, the top-mounted burner of the combustion rig is fed with cleaned and dried air, while a mix of CO_2 and O_2 from tanks is fed to simulate flue gas recycling for oxy-fuel operation. In this way, oxy-fuel recycle rates are highly flexible by adjusting the O_2

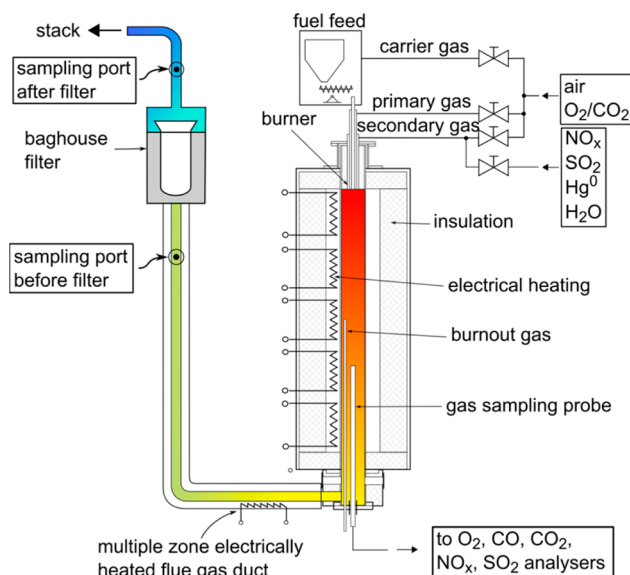


Figure 1. Schematic of the experimental combustion rig used for air and oxy-fuel investigations.

concentration in the oxidant. To simulate the flue gas recycle of an oxy-fuel process with impurities present in the recycled gas, the oxidant gas can be doped with desired amounts of NO_x , SO_2 , Hg^0 , and H_2O . This highly flexible method allows for an investigation of oxy-fuel combustion with simulation of different extents of recycle gas treatment (e.g., varying Hg^0 and SO_2 removal rates) and impurity concentrations in coal. With this approach, the impact of changing concentrations of individual flue gas components can be investigated over a wide range, which enables an understanding of the impurity behavior and coal-specific ash interactions.

Comprehensive Hg^0 and Hg^{2+} measurements were performed before and after the baghouse filter of the rig, to evaluate Hg oxidation and Hg removal in the filter. The baghouse filter was cleaned regularly to counteract a drop in the flue gas flow rate and therefore in the flue gas residence time in the system. To accomplish minimum possible differences of the ash loadings on the filter, even though the fuels used had considerably differing ash contents, the filter was cleaned before each Hg measurement was started. During the course of an individual measurement, the filter cleaning was discontinued. This implies an unavoidable increase of the ash loading of the baghouse filter during single measurements as well as differing ash buildup rates for different coal feed rates and coal ash contents. These conditions are however similar to a large-scale combustion system, where ash buildup rates vary with varying ash content and fuel feed rates. A separation of the parameters of ash loading on the filter and ash composition was not possible during the experiments with combustion of coals with highly differing characteristics and combustion conditions.

2.2. Hg^0 Gas Generator. A Hg^0 generator, working on a evaporation–condensation principle, was used for the injection of Hg^0 to the secondary oxidant stream (see Figure 2). Air is dosed with

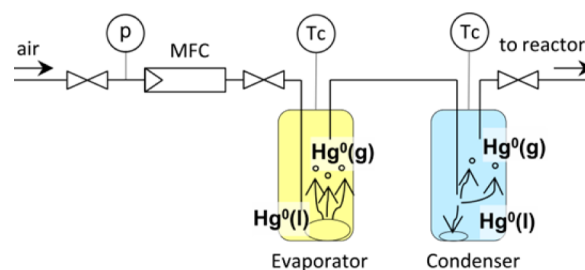


Figure 2. Schematic of the Hg^0 generator.

Table 1. Applied Gas Analyzers and Calibration Gases

species	measurement technique	manufacturer	calibration gases	
			air	oxy-fuel
O ₂	paramagnetism	ABB EL 3020	3 vol % in N ₂	3 vol % in CO ₂
CO ₂	NDIR	ABB EL 3020	16 vol % in N ₂	
		Siemens Ultramat 23		85 vol % in N ₂
SO ₂	NDIR	Siemens Ultramat 23	506 ppm in N ₂	506 ppm in N ₂
CO	NDIR	Siemens Ultramat 23	200 ppm in N ₂	200 ppm in N ₂
		ABB EL 3020	12 vol % in N ₂	12 vol % in N ₂

high accuracy to a heated, temperature-controlled Hg evaporation vessel containing metallic Hg⁰ using a mass flow controller (MFC). There, Hg⁰ is evaporated, generating a high Hg concentration in the gas. This gas is supplied to a highly accurate temperature-controlled Hg⁰ condensation vessel (± 0.05 K), which is set to a condensation temperature between 15 and 25 °C, where Hg⁰ condenses until the gas reaches its Hg⁰ saturation concentration at the set temperature. To calculate Hg⁰ concentrations in the gas exiting the condenser, an Antoine expression for the Hg vapor pressure with coefficients by Hicks⁴² was used. By setting up the gas flow rate and the condenser temperature of the system, the generated Hg mass flow was controlled. The system was tested under lab conditions in comparison to a certified Hg analyzer (SEMTECH Hg 2010) and proved to generate a Hg⁰ stream according to the predicting calculations with high accuracy. In a lab test, deviations between set and measured concentrations were in a range of $\pm 6.5\%$.

For experiments involving Hg⁰ injection, the system was set up at the start of the experiments and the Hg⁰ concentration in the oxidant gas was repeatedly checked by Hg measurements during a day's experiments. Generally, the set concentration was very stable.

2.3. Measurement and Sampling Equipment and Procedures. During the experimental campaigns, the gases O₂, CO₂, SO₂, NO_x, and CO were continuously sampled at the end of the furnace using a tempered oil-cooled (~ 180 °C) sampling probe and analyzed (analyzers and calibration gases; see Table 1). Reported H₂O concentrations were calculated on the basis of coal composition and water injection. Coals were analyzed for their calorific value (DIN 51900⁴³), proximate (DIN 51734,⁴⁴ DIN 51718,⁴⁵ DIN 51719,⁴⁶ and DIN 51720⁴⁷), and elemental (DIN 51732,⁴⁸ DIN 51724,⁴⁹ and DIN 51733⁵⁰) compositions, Cl (DIN 51727⁵¹) and Hg (DIN 22022⁵²) contents, and ash composition (DIN 51729⁵³). In all experiments, ash samples were extracted at the end of the furnace and from the baghouse filter of the combustion rig and were analyzed at IFK's laboratory for their contents of C in ash, S, and main ash-forming elements (according to standards DIN 51732,⁴⁸ DIN 51724,⁴⁹ and DIN 51729⁵³). During the experiments, SO₂ concentrations were measured based on the standard VDI 2462⁵⁴ before and after the baghouse filter of the combustion rig (detailed results will be published elsewhere). Moreover, HCl concentrations were measured applying standards DIN EN 1911⁵⁵ and DIN EN ISO 10304.⁵⁶

Measurements of elemental and total Hg in the gas phase (Hg⁰ and Hg^{tot}) were performed before (at approximately 350 °C) and after (at approximately 195 °C) the baghouse filter of the combustion rig using a continuous RA-915M Hg analyzer by Lumex, Ltd. that measures Hg⁰ based on a cold-vapor atomic absorption at 253.7 nm. This analyzer uses no amalgamation for the Hg measurement and, therefore, is not equipped with a MFC that was reported to cause biased Hg measurements if used with oxy-fuel flue gas.⁵⁷ In a lab experiment, the Lumex RA-915M analyzer was comparatively tested against a TÜV-certified⁵⁸ and approved SEMTECH Hg 2010 analyzer in a gas doped with different concentrations of Hg⁰ by the Hg generator described in section 2.2. The agreement between both analyzers was very good, as seen in Figure 3.

During sampling, the sampling port and probe were heated to 100–140 °C. To avoid disturbances of the measurement, all lines that were in contact with the sample gas were made of glass, perfluoroalkoxy (PFA), or polytetrafluoroethylene (PTFE). Because the Hg analyzer is only capable of measuring elemental Hg⁰, a sample gas conditioning

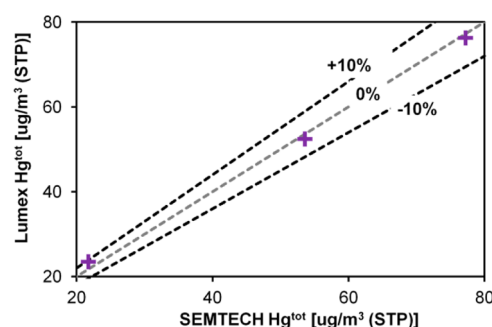


Figure 3. Comparative measurement of the Lumex RA-915M and a TÜV-certified SEMTECH Hg 2010 analyzer. Dashed lines show deviations of 0 and $\pm 10\%$ between the measurements.

system was applied to convert oxidized forms of Hg to Hg⁰ by contacting the gas with an aqueous 0.5 mol/L SnCl₂·H₂O/HCl reduction solution. This approach for Hg^{tot} measurements was successfully applied in the past at IFK by Hocquel⁵⁹ and similarly also by other institutes, such as EERC.⁶⁰ To maintain a high quality of the reduction solution, particularly at high SO₂ levels, the solution was not cycled but only used once. At high SO₂ concentrations, an accumulation of sulfur in the wet chemical sample gas conditioning system is possible and can interfere with the Hg measurement.⁶⁰ To reduce this accumulation, instead of contacting sample gas and SnCl₂ solution in impingers or glass coils with a relatively high internal volume and therefore residence time of the liquid, a co-current flow gas–liquid contacting reactor with minimized internal volume but similar gas liquid contact time was used. This setup was tested in comparison to a conventional sample gas conditioning system, measuring air that was doped with a constant concentration of Hg⁰ and varying SO₂ concentrations. The results of this test can be found in Figure 4.

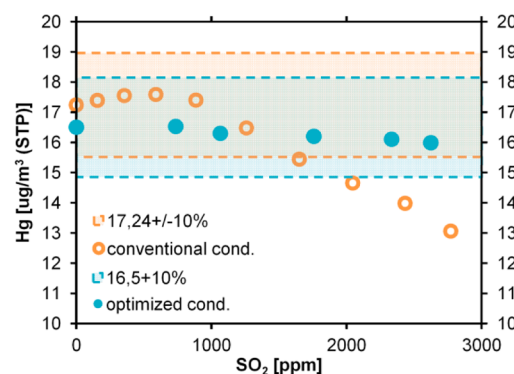


Figure 4. Impact of SO₂ on measured Hg^{tot} concentrations with conventional and optimized sample gas conditioning system measuring air that was doped with 17.24 and 16.5 $\mu\text{g}/\text{m}^3$ (STP) Hg⁰, respectively. Highlighted areas show deviations of $\pm 10\%$ from these concentrations.

With the optimized sample gas conditioning system, measured Hg^{tot} concentrations were only minimally impacted by SO_2 concentrations of levels to be expected in the planned oxy-fuel experiments. The deviation of measured and doped Hg concentrations with this system at a SO_2 concentration of 2623 ppm was only -3.1% , while with a conventional system, it was -24.2% at 2770 ppm SO_2 . A schematic of the sampling train for measuring Hg^{tot} is shown in Figure 5. As

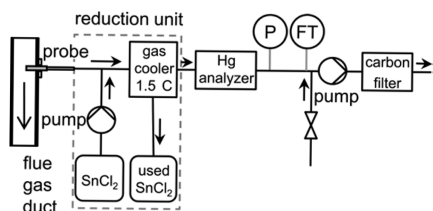


Figure 5. Schematic of the Hg sampling train.

reported in section 2.5, the recovery of Hg^{tot} introduced with fuel and Hg doping during combustion experiments was very good, which indicates a high accuracy of the performed Hg^{tot} measurements.

Similar to the experiments reported by Hocquel et al.,^{29,59} for measurements of elemental Hg in the flue gas, the sampling train was equipped with an additional Hg^{2+} trap (approximately 0.5 g of a pretreated ion-exchanger resin placed in a sorbent tube, as proposed by Metzger and Braun⁶¹) to knock out HgCl_2 selectively and quantitatively after the probe and before entering the Hg^{2+} reduction system. This Hg^{2+} trap was shown to remove more than 97% of HgCl_2 at the temperature ($110\text{--}140\text{ }^\circ\text{C}$) at which it was operated during the sampling.⁶¹ The absolute sorption capacity of a 0.5 g batch of sorbent in the sorbent tube can be estimated to about 5 mg of Hg^{2+} and is large compared to the Hg^{2+} amount supplied with the sample gas flow.⁵⁹ In the performed experiments, Hg^{2+} traps were exchanged regularly after a total sorption of not more than about 0.025 mg of Hg^{2+} to ensure a quantitative sorption of Hg^{2+} in all experiments. A more detailed description and discussion of the Hg speciation measurement method applied is given by Hocquel.⁵⁹

The in-stack filter for ash separation was changed between samplings to minimize the impact of filter ash on the measurements. From the measured concentrations of Hg^0 and Hg^{tot} (total Hg), the concentration of Hg^{2+} was calculated: $\text{Hg}^{2+} = \text{Hg}^{\text{tot}} - \text{Hg}^0$. Reported Hg^0 and Hg^{2+} concentrations represent averaged concentrations from an interval of approximately 5–10 min of stable and representative Hg measurement and are related to standard conditions (DIN 1343:⁶² 0 $^\circ\text{C}$ and 1 atm). Hg measurement intervals were considered stable if their relative standard deviation was lower than 20% for Hg concentrations up to $1\text{ }\mu\text{g}/\text{m}^3$ (STP), lower than 15% for Hg concentrations of $1\text{--}2\text{ }\mu\text{g}/\text{m}^3$ (STP), lower than 10% for Hg concentrations of $2\text{--}4\text{ }\mu\text{g}/\text{m}^3$ (STP), lower than 7% for Hg concentrations of $2\text{--}8\text{ }\mu\text{g}/\text{m}^3$ (STP), and lower than 5% for Hg concentrations higher than $8\text{ }\mu\text{g}/\text{m}^3$ (STP). A 5–10 min measurement interval was considered to be valid if the analyzer reading went to zero when applying zero gas to the sample gas conditioning train after disconnection from the flue gas sampling probe and if the measured average concentration after reconnection to the sampling probe was similar to the level during the initial measurement interval (i.e., difference $< \pm 5\%$).

For the evaluation of the experiments, it should be considered that applied Hg analyzer Lumex RA-915M has a resolution of $\pm 0.1\text{ }\mu\text{g}/\text{m}^3$ (STP), using the single-pass measuring cell. At low measured concentrations of $1\text{--}2\text{ }\mu\text{g}/\text{m}^3$ (STP) (particularly for coal C air and clean oxy-fuel experiments), the resolution of the analyzer is in a range of $\pm 5\text{--}10\%$ of the measured concentrations.

2.4. Coal Properties. To be able to compare results to previous studies, the three Australian coals (A, B, and C) used in this study came from similar mines as those previously tested by IHI³ but have some differences in properties because of the variations of the coals across the mine sites with time. The coals were shipped from Australia to IFK and then prepared and crushed for the experiments. Coal properties are listed in Tables 2 and 3.

The coals differ considerably in their ash and sulfur contents. The ash contents of coals A, B, and C are in a proportion of roughly 3:2:1, while the S contents are in a proportion of about 1:2:2. The Cl contents of all three coals are low, with coal C having the highest Cl content of 0.017 wt %. When Fe contents referring to raw coals are calculated, coal A has the highest content with 1.55 wt %, followed by coals C and B with contents of 0.3 and 0.09 wt %, respectively. The high ash coals A and B are rich in Al and Si but relatively low in alkaline and earth alkaline elements (Ca, Mg, K, and Na). In contrast, coal C contains considerably higher contents of those elements.

2.5. Combustion Conditions. The investigated combustion conditions comprise of one conventional air-firing and seven different oxy-fuel combustion settings. The differences between the oxy-fuel experiments can be found in the injection rates of the flue gas impurities H_2O , NO, SO_2 , and Hg^0 . By variation of the injection, different removal rates of the impurities from the recycled gas between 0 and 100% were simulated. The removal rates refer to calculated, theoretical concentration maxima for H_2O , SO_2 , and Hg in an oxy-fuel process without any impurity removal and an exit O_2 concentration y_{O_2} of 3 vol % (dry), according to eqs 6 and 7.

$$y_{i,\text{max, oxy}} = \frac{\frac{y_i}{M_{\text{M},i}} \times 10^6}{\left(\frac{y_{\text{S}}}{M_{\text{M},\text{S}}} + \frac{y_{\text{C}}}{M_{\text{M},\text{C}}} + \frac{y_{\text{N}}}{2M_{\text{M},\text{N}}} \right) \frac{100}{100 - y_{\text{O}_2}}} \quad (6)$$

$$y_{\text{H}_2\text{O},\text{max, oxy}} = \frac{\left(\frac{y_{\text{H}}}{2M_{\text{M},\text{H}}} + \frac{y_{\text{W}}}{M_{\text{M},\text{W}}} \right) \times 10^2}{\left[\left(\frac{y_{\text{S}}}{M_{\text{M},\text{S}}} + \frac{y_{\text{C}}}{M_{\text{M},\text{C}}} + \frac{y_{\text{N}}}{2M_{\text{M},\text{N}}} \right) \frac{100}{100 - y_{\text{O}_2}} \right] + \frac{y_{\text{H}}}{2M_{\text{M},\text{H}}} + \frac{y_{\text{W}}}{M_{\text{M},\text{W}}}} \quad (7)$$

In total, six different settings with injection of H_2O , NO, SO_2 , and Hg^0 and one “clean oxy-fuel” configuration (labeled as OC) in which the fuels were combusted in a mix of pure O_2 and CO_2 (e.g., removal of 100% of all impurities) were investigated. In the other oxy-fuel experiments, the H_2O removal rate was fixed at approximately 20% and a constant concentration of NO (approximately 1000 ppm) in the recycled flue gas was simulated, while SO_2 removal rates of approximately 50, 20, and 0% and Hg removal rates of approximately 80, 50, and 0% were investigated.

All experiments are labeled with a code, allowing for identification of the experimental setting; e.g., C-O2SSH indicates an experiment with coal C (index: C) under oxy-fuel conditions (index: O) with

Table 2. Net Calorific Value (NCV), Proximate, Elemental, Cl, and Hg Analyses of the Investigated Australian Coals (Percentages on a Weight Basis)

coal	NCV ^a (kJ/kg)	W ^b (%, ad)	A ^c (%, db)	V ^d (%, daf)	FC ^e (%, daf)	C (%, daf)	H (%, daf)	N (%, daf)	S (%, daf)	O ^f (%, daf)	Cl (%, daf)	Hg (mg/kg, daf)
A	18026	3.9	32.5	35.9	64.1	73.8	4.3	1.1	0.3	20.5	nd ^g	0.07
B	24956	1.5	23.0	50.6	49.4	78.3	6.7	1.1	0.7	13.2	0.014	0.04
C	26748	3.7	9.84	35.9	64.1	77.2	5.2	2.0	0.7	15.0	0.017	0.02

^aNet calorific value. ^bWater. ^cAsh. ^dVolatile matter. ^eFixed carbon. ^fCalculated by difference. ^gNot determinable ($< 0.008\%$, daf).

Table 3. Analysis of Coals by Inductively Coupled Plasma–Optical Emission Spectroscopy (ICP–OES) for Main Ash-Forming Elements^a

coal	SiO ₂ (wt %)	Al ₂ O ₃ (wt %)	Fe ₂ O ₃ (wt %)	CaO (wt %)	MgO (wt %)	SO ₃ (wt %)	K ₂ O (wt %)	Na ₂ O (wt %)	TiO ₂ (wt %)	P ₂ O ₅ (wt %)
A	58.9	26.2	6.8	1.2	0.7	3.0	0.4	0.1	2.4	0.2
B	64.4	21.5	1.2	0.4	0.7	7.2	0.4	0.2	3.9	0.0
C	33.2	23.0	11.4	7.0	1.8	22.7	0.9	1.3	1.2	1.8

^aOn the basis of a direct analysis of raw, unmilled coal samples for ash-forming minerals, without previous ashing.

Table 4. List of All Experimental Settings and Simulated Removal Rates

		experimental settings				
		simulated capture rates (%)				
index	coal	air/oxy	H ₂ O	SO ₂	Hg	simulated NO concentration in recycled flue gas (ppm, dry)
A-A	A	air				
A-OC		Oxy28, clean	100	100	100	
A-O2SSH		Oxy28	23	23	44	962
A-O5SSH		Oxy28	23	52	44	962
A-O2S8H		Oxy28	23	23	79	962
A-O0SSH		Oxy28	23	4	44	962
A-O2S0H		Oxy28	23	23	7	962
A-O0S0H		Oxy28	23	4	7	962
B-A	B	air				
B-OC		Oxy28, clean	100	100	100	
B-O2SSH		Oxy28	24	24	51	949
C-A	C	air				
C-OC		Oxy28, clean	100	100	100	
C-O2SSH		Oxy28	23	23	62	959

Table 5. List of the Oxidant Composition (Balance in Air Experiments is N₂), the Simulated Recirculation Rate, and the Coal Mass Flows for All Experiments

index	recirculation rate (%)	coal mass flow (kg/h)	oxidant composition						
			O ₂ (vol %, wet)	O ₂ (vol %, dry)	CO ₂ (vol %, dry)	H ₂ O (vol %, wet)	SO ₂ (ppm, dry)	NO (ppm, dry)	Hg [$\mu\text{g}/\text{m}^3$ (STP), dry]
A-A		2.1	21.0	21	0	0	0	0	0
A-OC		2.8	28.0	28	72.0	0	0	0	0
A-O2SSH	72.6	2.8	33.7	28	66.3	16.9	824	654	17.8
A-O5SSH	72.6	2.8	33.7	28	66.3	16.9	515	654	17.8
A-O2S8H	72.6	2.8	33.7	28	66.3	16.9	824	654	6.5
A-O0SSH	72.6	2.8	33.7	28	66.3	16.9	1030	654	17.8
A-O2S0H	72.6	2.8	33.7	28	66.3	16.9	824	654	29.4
A-O0S0H	72.6	2.8	33.7	28	66.3	16.9	1030	654	29.4
B-A		1.5	21.0	21	0	0	0	0	0
B-OC		2.1	28.0	28	72.0	0	0	0	0
B-O2SSH	73.5	2.1	35.2	28	64.8	20.5	1569	631	8.9
C-A		1.4	21.0	21	0	0	0	0	0
C-OC		1.9	28.0	28	72.0	0	0	0	0
C-O2SSH	73.4	1.9	34.1	28	65.9	17.8	1723	648	3.8

simulated removal of 20% of the SO₂ (index: 2S) and 50% of the Hg (index: 5H) from the recycled gas. Coals A, B, and C were all tested under A, OC, and O2SSH conditions, and coal A was investigated with five additional oxy-fuel settings. Table 4 lists the experimental settings and removal rates in detail, while Table 5 summarizes information on oxidant compositions, simulated recirculation rates, and coal feeds. Slight deviations from the desired removal rates in Table 4 can be observed, but experiments with different coals and similar removal rates are considered comparable.

In the air combustion, the O₂ concentration of the oxidant was 21 vol % (wet), while for all oxy-fuel experiments, it was fixed at 28 vol % (wet), which corresponds to recycle rates of about 70%. The exit O₂ concentration was kept constant at 3 vol % (dry) for all experiments, implying somewhat differing combustion stoichiometries for the

different settings, because of the different concentrations of diluting N₂/CO₂ in the oxidant and different concentrations of H₂O in the flue gases at different experimental settings (approximately $1.09 < \lambda < 1.16$, where λ is the stoichiometric ratio of combustion).

2.6. Quality Assurance: Hg^{tot} Recovery Rates. To evaluate the significance of the performed experiments, mass balance calculations for Hg^{tot} were performed on the basis of the input of Hg with fuel and Hg⁰ injection and a good agreement to gaseous Hg^{tot} concentrations measured before filter (~ 350 °C) was obtained (see Figure 6). The deviations of measured and theoretical concentrations of Hg^{tot} calculated on the basis of a Hg mass balance of the rig were in a range between approximately -11 and 1% for experiments simulating Hg⁰ recycle. It should be noted that higher deviations for air and clean oxy-fuel experiments with coals A and B might be due to the limited

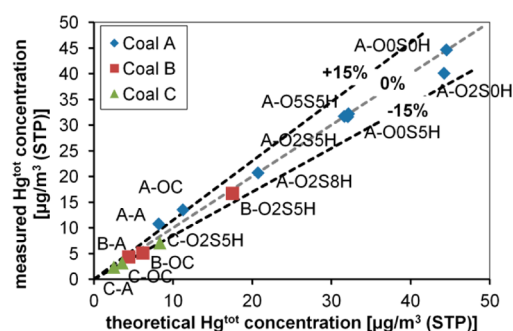


Figure 6. Theoretical Hg^{tot} concentrations versus Hg^{tot} concentrations measured before filter (350 °C) for coal A (diamonds), B (squares), and C (triangles) experiments. The gray dashed line represents 0% deviation between measured and calculated values, while black dashed lines mark a range of $\pm 15\%$ deviation.

accuracy of the Hg analysis of the coal. In DIN 22022-6,⁶³ the standard used for Hg analyses, a relative standard deviation of 20.3% is given that was obtained for repetitive Hg analyses of hard coal from a round-robin test.

3. RESULTS

3.1. Flue Gas Composition. Table 6 lists the measured/calculated concentrations of O_2 , SO_2 , H_2O , SO_3 , and HCl. The concentrations of O_2 and SO_2 represent mean values calculated on the basis of a minimum of 10 min of relatively stable, representative operation. The O_2 concentrations were kept relatively stable around 3 vol % (2.8–3.6 vol %, dry). During all oxy-fuel experiments, CO_2 concentrations higher than 95 vol % (dry) were reached, proving a minimum amount of air ingress to the system. All mean CO concentrations were below 90 ppm (<25 ppm in most cases). Different fuel sulfur contents and different fuel feed rates between air (A) and oxy-clean (OC) combustion are directly represented in differences in the measured concentrations of SO_2 . Measured SO_3 concentrations seem to be influenced by SO_2 concentrations and ash composition. HCl concentrations during all experiments are low (<10 ppm), as expected on the basis of the low Cl content of the coals.

3.2. Composition of Ash Samples. The UBC contents of all baghouse filter ashes involving coal C were low (0.1–0.75%), and those from coals A and B were below the detection limit of 0.1%. This illustrates that all UBC contents were at similar, low levels and that the influence of variations in the UBC content on the measured Hg concentrations may be limited. Ash, Hg and S contents were close to or below the detection limit. Because of the high variability of the analyses in that range, the possibilities to evaluate this data are limited. A trend that can be found in most of the analyses is that sulfur contents measured in the samples from the baghouse filter are slightly higher than those of samples from the end of the

furnace. This trend of an increase may be connected to SO_3 capture on the ash in the filter. A comparison of the composition of sampled ash (analysis for main ash-forming elements) from the air (A), clean oxy-fuel (OC), and the O2S5H experiments reveals that differences between the different experimental settings are minimal. The distribution of elements in the ash samples from the baghouse filter and the furnace represents the composition of the ashes of the raw coals.

3.3. Hg^0 and Hg^{2+} Concentrations. Figure 7 shows the mean concentrations of Hg^0 and Hg^{2+} measured before and

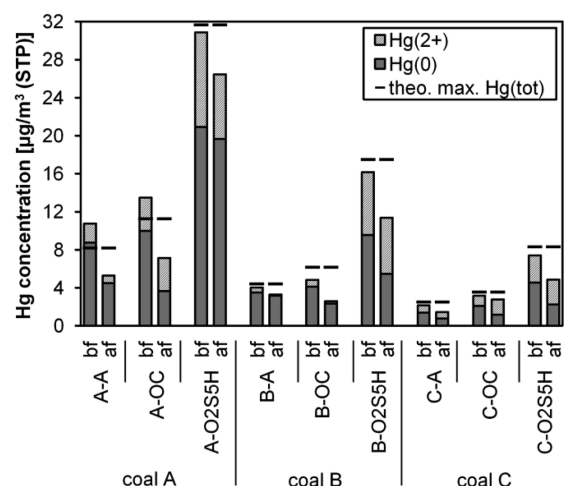


Figure 7. Hg^0 (solid) and Hg^{2+} (hatched) concentrations measured before (bf) and after (af) the baghouse filter and theoretically calculated maximum concentrations for coal A, B, and C experiments.

after the baghouse filter as well as the theoretically possible maximum Hg^{tot} concentrations for the air, clean oxy-fuel, and O2S5H experiments for all three investigated coals. Figure 8 shows the same for additional oxy-fuel experiments with coal A. In Figure 7, differences in the measured Hg concentrations can be observed that were expected on the basis of the differences of the Hg contents of the coals, with coal A having the highest Hg emissions and coal C having the lowest. When the combustion conditions are compared, one observes that not only the O2S5H settings with Hg doping of the oxidant gas but also the clean oxy-fuel experiments show higher Hg^{tot} concentrations than the air combustion. The reason for this is the higher oxidant O_2 content in the clean oxy-fuel experiment (28 vol %) that requires a higher fuel feed to keep a constant excess O_2 level of the combustion at a constant flue gas production rate.

In all performed experiments (Figures 7 and 8), one observes lower Hg^{tot} concentrations at the filter outlet, than at the inlet, because of Hg capture on the ash at the filter. In Figure 8, the

Table 6. O_2 , H_2O , SO_2 , SO_3 , and HCl Concentrations Measured/Calculated^a

index	A-A	A-OC	A-O2S8H	A-O5S5H	A-O2S5H	A-O0S5H	A-O2S0H	A-O0S0H	B-A	B-OC	B-O2S5H	C-A	C-OC	C-O2S5H
O_2 (vol %, dry) ^b	3.0	3.4	3.0	3.1	3.6	3.2	2.7	2.9	3.1	3.2	3.0	3.1	2.8	3.1
H_2O (vol %, wet) ^b	6.4	8.7	23.5	23.5	23.5	23.5	23.5	23.5	7.6	10.4	28.5	6.6	9.1	24.3
SO_2 (ppm, dry) ^b	199	283	1228	871	1235	1464	1243	1531	367	498	2578	444	603	2802
SO_3 (ppm, dry) ^c	1.3	5.7	28.0	16.0	24.1	37.0	28.1	36.8	8.3	19.7	52.5	0.2	0.5	36.5
HCl (ppm, dry) ^c	4	3	4	4	4	4	4	4	3	5	7	6	8	9

^a H_2O concentrations calculated on the basis of the fuel composition and steam injection to the oxidant gas. ^bAt end of the furnace. ^cBefore filter.

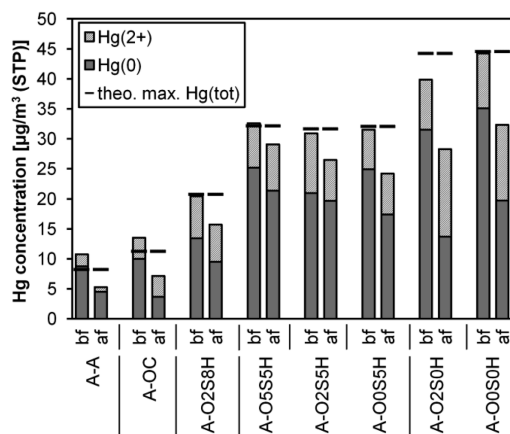


Figure 8. Hg^0 (solid) and Hg^{2+} (hatched) concentrations measured before (bf) and after (af) the baghouse filter and theoretically calculated maximum concentrations for coal A experiments.

impact of the simulated Hg recycle on measured Hg concentrations is obvious. For example, an oxy-fuel combustion with complete removal of Hg from the recycled flue gas (A-OC) would lead to a 3.3-fold decrease in the Hg concentrations before filter and a 4.5-fold decrease after filter compared to a recycle configuration without any Hg removal (A-O0S0H).

3.4. Hg Speciation. The percentaged speciation of the Hg emissions between Hg^0 and Hg^{2+} measured before and after the baghouse filter for the air, clean oxy-fuel, and O2SSH experiments for all three investigated coals are shown in Figure 9. Figure 10 shows the same for additional oxy-fuel experiments

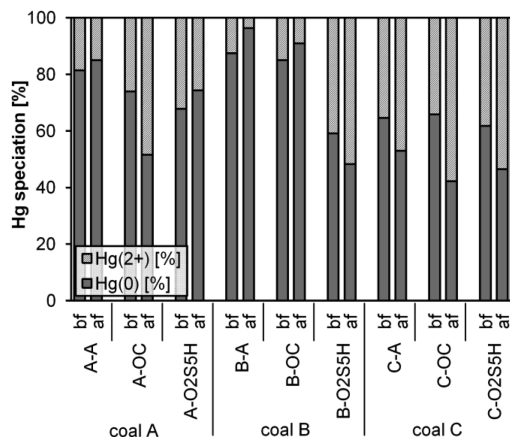


Figure 9. Percentaged speciation between Hg^0 (solid) and Hg^{2+} (hatched) before (bf) and after (af) the baghouse filter for coal A, B, and C experiments.

with coal A. The results for the three different coals reveal that a switch from air to oxy-fuel combustion with impurity recycling leads to an increased $\text{Hg}^{2+}/\text{Hg}^{\text{tot}}$ ratio at the sampling locations before as well as after the baghouse filter. Coals A, B, and C have a different Hg speciation behavior. Coal C that is lowest in Hg and highest in Cl, with comparatively high contents of Fe and Ca in the ash, shows the highest conversion of Hg into Hg^{2+} . Coal B that is higher in S and lower in Fe and Ca in the ash shows lower Hg^{2+} formation than coal A in air and clean oxy-fuel experiments. Conversely, coal B seems to be the only one of the investigated fuels for which the increase of the SO_2 concentrations in the O2SSH experiment fundamen-

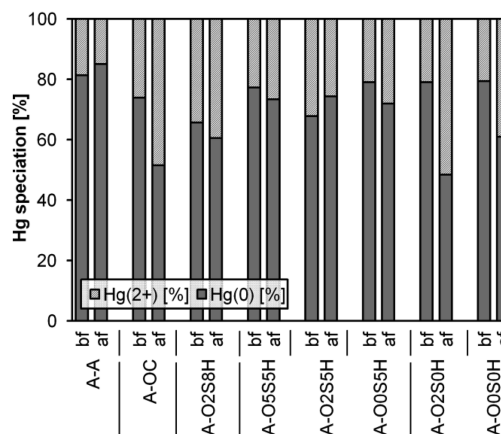


Figure 10. Percentaged speciation between Hg^0 (solid) and Hg^{2+} (hatched) before (bf) and after (af) the baghouse filter for coal A experiments.

tally increases the Hg oxidation, while for coals A and C, this increase is less pronounced. When looking at the results in Figures 9 and 10, one sees the trend that, in almost all experiments with relatively high proportions of Hg^{2+} (>25%) at the sampling location before filter, this proportion is even increasing, when flue gases pass the filter, while in all experiments with low proportions of Hg^{2+} (<25%) found before the filter, Hg^{2+} proportions are decreasing.

3.5. Hg Capture in the Baghouse Filter. In Figures 11 and 12, the Hg^0 , Hg^{2+} , and Hg^{tot} capture efficiencies for all

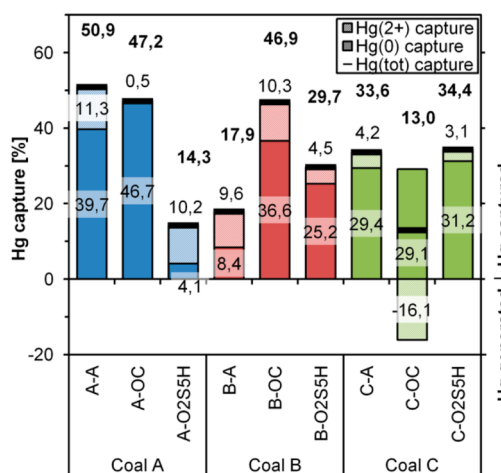


Figure 11. Hg^0 (solid), Hg^{2+} (hatched), and Hg^{tot} (black line and bold print) capture on the baghouse filter for coal A, B, and C experiments.

performed experiments are shown. The capture efficiencies were calculated according to eq 8.

$$\eta_{\text{Hg},l} = \frac{c_{\text{Hg},l,\text{bf}} - c_{\text{Hg},l,\text{af}}}{c_{\text{Hg},\text{tot},\text{bf}}} \times 100\% \quad (8)$$

Hg^{tot} capture efficiencies on the baghouse filter between 18 and 51% were found for air combustion, while for clean oxy-fuel combustion, capture efficiencies were between 13 and 47%. For coals A and C, the capture efficiencies decreased when switching from air to the clean oxy-fuel combustion conditions, while for coal C, the behavior was opposite. In oxy-fuel combustion with impurity recycling (i.e., O2SSH experiments),

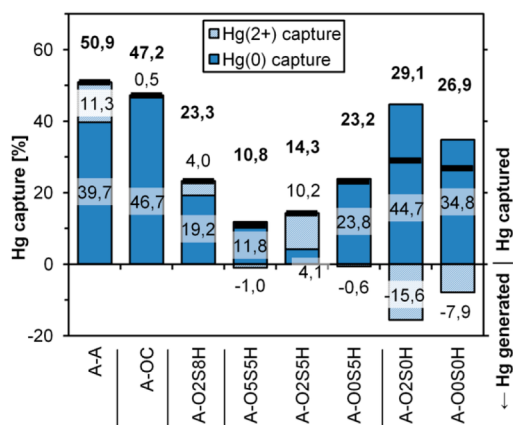


Figure 12. Hg^0 (solid), Hg^{2+} (hatched), and Hg^{tot} (black line and bold print) capture on the baghouse filter for coal A experiments.

Hg^{tot} capture was between 10 and 34%. When comparing capture efficiencies of air and O2SSH experiments, no clear trend is obvious: for coal A, capture decreases; for coal B, it increases; and for coal C, it remains at a similar level.

Negative capture efficiencies for Hg^{2+} at the baghouse filter were found for some experiments and can be interpreted as an overall Hg^0 oxidation at this unit, creating higher Hg^{2+} concentrations at the filter outlet than at the inlet. Such an effect was mainly observed for experiments with simulated Hg and SO_2 recycling. Hg^0 concentrations decreased in all experiments, when flue gases passed the baghouse filter.

4. DISCUSSION

The extent of the available experimental data from air and, in particular, oxy-fuel experiments with three different coals allows for an evaluation of parameters that influence Hg speciation and Hg interactions with fly ash on a baghouse filter (oxidation and capture) in the firing system. Because of the scale and the nature of the performed experiments, it is however not possible to separate the impacts of all parameters that potentially influence the Hg transformation in the system (e.g., SO_2 and SO_3 , ash content, ash composition, and Hg levels).

4.1. Impact of Experimental Conditions on Hg Speciation. Switching from air to “clean oxy-fuel” conditions (without impurity injection) offers an opportunity to compare the effect of firing under higher oxidant O_2 concentrations, which, in turn, increased the coal-derived impurity levels by about 40%. Under these conditions, the $\text{Hg}^{2+}/\text{Hg}^{\text{tot}}$ ratio was observed to increase by 7.5, 2.6, and -1.2% for coals A, B, and C (absolute percentage changes, before filter). This suggests a mixed response for different coals, which may be ash-related. The simulation of hot oxy-fuel recycle conditions (through impurity injection) allows for an investigation of the effect of higher impurity concentrations without changes to residence time or dust loading. Under these conditions, all three coals showed a further increase in oxidized Hg in the order of 6.1, 25.8, and 4.1% for coals A, B, and C, respectively (absolute percentage changes, before filter). The degree of Hg oxidation ($\text{Hg}^{2+}/\text{Hg}^{\text{tot}}$ ratio) was observed to be correlated to the SO_2 and/or SO_3 concentrations in the flue gas, as seen from correlation factors in Table 7. The correlation is strong for coals B and C and less significant for coal A. With increasing SO_2 (Figure 13) as well as SO_3 (Figure 14) concentrations, the $\text{Hg}^{2+}/\text{Hg}^{\text{tot}}$ ratio before filter is increasing. For coal A, the effect seems more pronounced at the filter outlet, as seen in Figure 15

Table 7. Pearson Product-Moment Correlation Coefficients (Pearson's r) for the Correlations between the Hg Oxidation ($\text{Hg}^{2+}/\text{Hg}^{\text{tot}}$ Ratio) before (bf) and after (af) Filter and the SO_2 (End of Furnace) and SO_3 (before Filter) Concentrations

correlation		Pearson's r		
		coal A	coal B	coal C
$\text{Hg}^{2+}/\text{Hg}^{\text{tot}}$ ratio, bf	SO_2	0.16	1.00	0.94
$\text{Hg}^{2+}/\text{Hg}^{\text{tot}}$ ratio, bf	SO_3	0.09	0.99	
$\text{Hg}^{2+}/\text{Hg}^{\text{tot}}$ ratio, af	SO_2	0.21	1.00	0.18
$\text{Hg}^{2+}/\text{Hg}^{\text{tot}}$ ratio, af	SO_3	0.26	0.99	

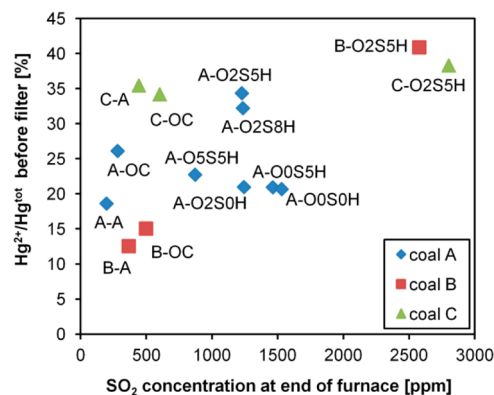


Figure 13. SO_2 concentrations (end of furnace) versus $\text{Hg}^{2+}/\text{Hg}^{\text{tot}}$ ratios “before filter” for coal A (diamonds), B (squares), and C (triangles) experiments.

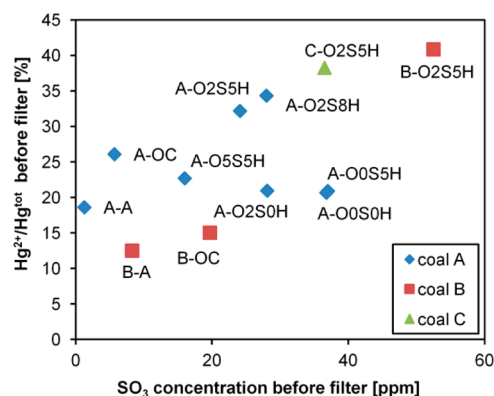


Figure 14. SO_3 concentrations (before filter) versus $\text{Hg}^{2+}/\text{Hg}^{\text{tot}}$ ratios “before filter” for coal A (diamonds), B (squares), and C (triangles) experiments.

(results for SO_3 are not shown but similar) and Table 7. An improvement of the homogeneous and/or heterogeneous Hg oxidation on fly ash by SO_2 and/or $\text{SO}_3/\text{H}_2\text{SO}_4$ may explain the observed behavior. Possible effects of SO_2 and $\text{SO}_3/\text{H}_2\text{SO}_4$ on Hg oxidation were discussed by others.^{12,28,33,36}

4.2. Impact of the Ash Content on Hg Capture. One observation that was made is that the theoretically calculated Hg^{tot} concentration to be in the flue gas matches very well with the Hg^{tot} concentrations measured in the flue gas before filter at approximately 350 °C for all runs. This indicates that the entrained fly ash at temperatures greater than approximately 350 °C has no impact on mercury capture (other than through Hg oxidation). It is also important to note that the combustion tests resulted in almost 100% combustion, leaving less than 1%

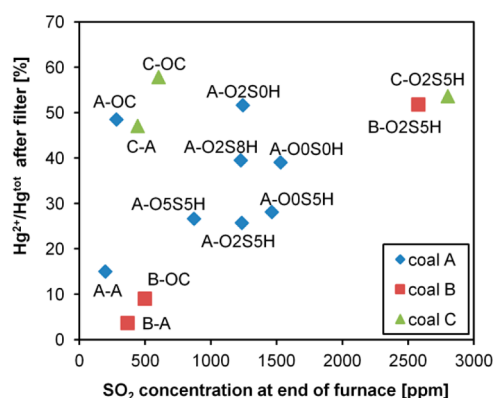


Figure 15. SO_2 concentrations (end of furnace) versus $\text{Hg}^{2+}/\text{Hg}^{\text{tot}}$ ratios "after filter" for coal A (diamonds), B (squares), and C (triangles) experiments.

unburned carbon in the fly ash. Because unburned carbon in the ash is expected to have a significant Hg capture potential, these results are unique in producing a predominantly inorganic mineral effect on Hg capture. Figure 16 shows the dependency

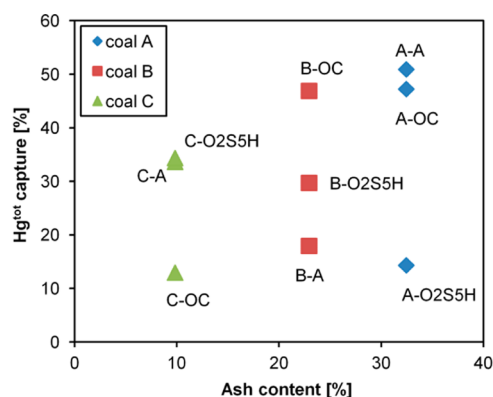


Figure 16. Coal ash content versus Hg^{tot} capture for coal A (diamonds), B (squares), and C (triangles) experiments.

of the Hg^{tot} capture at the baghouse filter for the air, clean oxy-fuel, and O2SSH experiments with coals A, B, and C versus the ash contents of the coals. In the plot, a clear correlation between ash contents and Hg capture cannot be determined. Other factors, such as the differing flue gas compositions in combination with differing ash compositions also have a considerable effect on the Hg capture that may be overlaying the impact of the ash content.

4.3. Impact of Experimental Conditions on Hg Capture. Figures 17 and 18 visualize the relation between the Hg^{tot} concentration at the baghouse filter inlet and the capture of Hg^{tot} and Hg^{2+} at the filter for coal A experiments. At high Hg^{tot} concentrations at the filter inlet in oxy-fuel experiments with simulated Hg^0 and SO_2 recycling, decreased Hg^{tot} capture efficiencies at the filter can be observed in comparison to the air and clean oxy-fuel experiments. Such behavior may be a mixed reply to high Hg^0 and SO_2 and SO_3 concentrations. Possibly, a kinetic limitation of one or more of the steps involved in the capture of Hg on the ash (e.g., Hg^0 and Hg^{2+} physisorption, Hg^0 oxidation, and Hg^{2+} chemisorption³⁰) or a physical limitation of available sorption sites causes the effect. The increased SO_2 and SO_3 concentrations in the experiments with impurity recycling are likely responsible for a

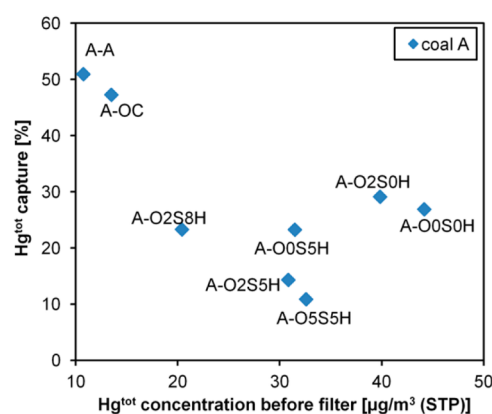


Figure 17. Hg^{tot} concentration before filter versus Hg^{tot} capture for coal A experiments.

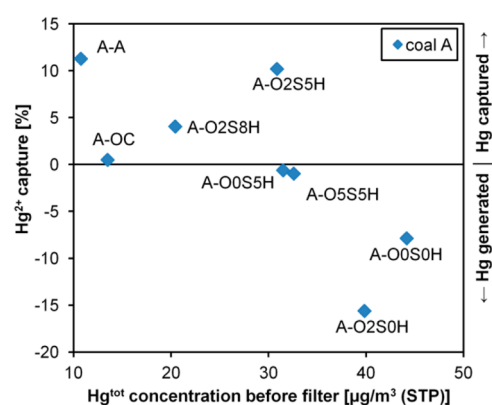


Figure 18. Hg^{tot} concentration before filter versus percentage of Hg^{2+} capture at the filter related to the Hg^{tot} concentration at the filter inlet for coal A.

depletion of Hg sorption sites on the ash (also see the explanation of Figure 19).

In Figure 18, one observes that, with increasing Hg^{tot} concentrations at the filter inlet, the filter changes from being a Hg^{2+} capture unit to a Hg^{2+} generator. This behavior is at least partially responsible for the low Hg^{tot} capture efficiencies (Figure 17) and the increased degree of Hg oxidation (Figure 13) under oxy-fuel conditions with simulated Hg^0 and SO_2 recycle. For the Hg^{2+} capture, the Hg^0 physisorption and oxidation are possibly not limiting but instead the Hg^{2+} chemisorption. Either a kinetic limitation of this chemisorption, or more likely a limited availability of sorption sites of coal A (low UBC), or a combination of both can explain the behavior. The availability of sorption sites may be reduced because of their consumption by high amounts of SO_2 and SO_3 under oxy-fuel conditions with impurity recycling. In both cases, an increase of the availability of sorption sites for HgCl_2 (e.g., by sorbent injection) may improve the Hg^{2+} capture performance at the filter considerably.

Figure 19 shows how the measured SO_3 concentrations at the filter inlet are related to the Hg^{tot} capture efficiencies of this unit for oxy-fuel experiments with simulated Hg^0 and SO_2 recycling. Experiments with impurity recycling show lower Hg capture on ash than air and clean oxy-fuel experiments. Likely, the increased SO_2 and SO_3 concentrations in the experiments with impurity recycling lead to a depletion of Hg sorption sites on the ash and cause the lower Hg capture. However, the Hg^{tot}

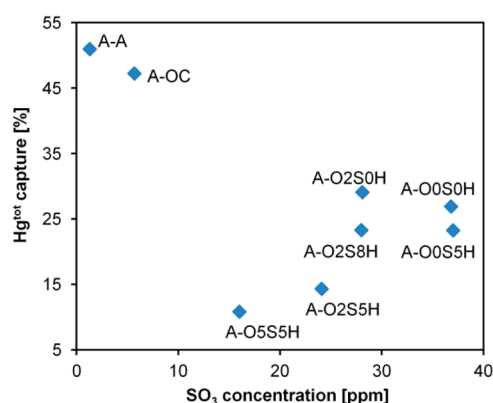


Figure 19. SO₃ concentration before filter versus Hg^{tot} capture for coal A experiments.

capture efficiencies in experiments with impurity recycling and, therefore, considerably higher SO₃ concentrations compared to the air and clean oxy-fuel experiments show a positive correlation between SO₃ levels at the filter inlet and Hg^{tot} capture. Considering the low unburned carbon content of filter ashes of the high-ash coal A, possibly not only carbon sorption sites play a role in the capture of Hg but also mineral species.^{12,64} The Hg^{tot} capture on the ash may profit from the improved Hg oxidation at higher SO₃/H₂SO₄ concentrations^{12,31} and also from an acidification of the ash.⁶⁴ In Hg sorption experiments on pure, temperature-controlled minerals, Jäger et al. showed that the Hg capture on CaO and MgO was improved when adding 250 ppm SO₂ to the gas mix (N₂-based gases).^{64,65} However, the effects of SO₃ and higher SO₂ concentrations on Hg sorption on CaO and MgO or other Ca- and Mg-bearing ash minerals were not investigated in their experiments.

5. SUMMARY AND CONCLUSIONS

A comprehensive study on the Hg oxidation and capture behavior of three Australian coals under air and simulated oxy-fuel conditions with variable degrees of flue gas cleaning was performed at IFK, University of Stuttgart. To simulate different extents of oxy-fuel flue gas cleaning in a once-through system, the CO₂/O₂ oxidant mix was doped with SO₂, H₂O, NO, and Hg⁰. The Hg recovery of the experimental system under oxy-fuel conditions with impurity recycling was very good, with deviations between Hg^{tot} mass balance and Hg^{tot} concentrations measured before filter (~350 °C), below 11%.

An increase in Hg^{tot} was observed when switching from air to “clean oxy-fuel” conditions, which was concurrent with the higher O₂ in the oxidant. Under air combustion conditions, Hg^{tot} concentrations before the baghouse filter of 2.2, 4.0, and 10.7 μg/m³ (STP) were measured for coals A, B, and C, respectively, while in oxy-fuel combustion with Hg and SO₂ recycling (2SSH experiments), values of 7.4, 16.2, and 30.8 μg/m³ (STP) were found. Differences between the coals in the measured Hg concentrations represent the different Hg contents of the coals and highlight the importance of this parameter on the Hg concentrations in air and oxy-fuel combustion systems.

The three coals show differences in their Hg oxidation behavior that can be connected to their different compositions. A switch from air to oxy-fuel combustion with impurities recycling leads for all three investigated coals to an increased Hg²⁺/Hg^{tot} ratio at the sampling locations before as well as after

the baghouse filter. An absolute increase of the Hg²⁺/Hg^{tot} ratio of up to 28.3% before filter and up to 48.1% after filter was found when comparing oxy-fuel-firing conditions with impurity recycling to air combustion conditions. In almost all experiments, the Hg²⁺ share in the flue gas increased when the flue gas passes through the baghouse filter of the experimental rig. In a few experiments with high Hg^{tot} concentrations at the filter inlet, this is associated with an increase of the Hg²⁺ concentrations at the filter outlet. Possibly, this is a mixed reply to high Hg⁰ and SO₂ and SO₃ concentrations. The capture of Hg²⁺ in these cases may be limited by kinetics of the Hg²⁺ chemisorption on the ash and/or the availability of Hg²⁺ sorption sites. The increased SO₂ and SO₃ concentrations in the experiments with impurity recycling are likely responsible for a depletion of Hg sorption sites on the ash.

Under all experimental conditions, considerable amounts of Hg were captured when the flue gas passed through the ash in the baghouse filter. Capture efficiencies between 18 and 51% were measured under air-fired conditions, while under oxy-fuel conditions, capture efficiencies between about 11 and 29% were found. Possibly, higher Hg, SO₂ and SO₃ concentrations than in the air and clean oxy-fuel experiments are responsible for reduced Hg capture efficiencies under oxy-fuel conditions with impurity recycling.

Higher Hg concentrations and, for some coals, a decreased baghouse filter Hg capture performance in oxy-fuel combustion illustrate that a better understanding of Hg emission behavior and reduction technologies is crucial to limit the Hg concentrations in oxy-fuel flue gases to levels that are tolerable for flue gas processing in CO₂ liquefaction units. Future investigations may reveal the detailed mechanisms involved in homogeneous and heterogeneous Hg oxidation and Hg capture under oxy-fuel conditions and should also investigate the effect of variations in the flue gas temperature-residence time profile that can occur when switching from air to oxy-fuel combustion in industrial-scale applications. The higher levels of Hg oxidation, observed under “hot” recycle conditions (e.g., experiments with impurity injection), suggest that a greater portion of the total gas-phase Hg can be removed with the ash and during flue gas quenching prior to compression. Moreover, it is expected that further significant removal would occur in a practical bag filter where higher unburned carbon levels are encountered than in the performed experiments. Additive technologies that enhance the oxidation rate of gaseous Hg⁰ and the capture of Hg on ash (e.g., activated carbon injection) can ultimately reduce the amount of Hg entering the compression system and reduce the need for dedicated Hg capture beds.

■ AUTHOR INFORMATION

Corresponding Author

*E-mail: reinhold.spoerl@ifk.uni-stuttgart.de.

Notes

The authors declare no competing financial interest.

■ ACKNOWLEDGMENTS

The authors gratefully acknowledge the financial support from Xstrata Coal Low Emissions R&D Corporation Pty Ltd. for a subcontract from the Project CC08-71 on “Coal Impurity Impacts and Gas Quality Control in Oxy-fuel Technology for CCS” conducted at the University of Newcastle, Australia. The authors also thank C. Ndibe, M. Pagano, and J. Walker of IFK’s

department “Firing Systems” and W. Ross and his team of IFK’s “Laboratory for Fuels, Ashes and Slag” for their support in the performed experiments as well as S. Farr, T. Schwämmle, and B. Heidel of IFK’s department “Fuels and Flue Gas Cleaning” for their invaluable advice and support with questions related to Hg measurements. Thanks also go to J. Spörl and A. Scheyhing for their support with the construction of a Hg⁰ gas generator

NOMENCLATURE

$y_{i,\max,oxy}$ = maximum volumetric concentration of component i in the oxy-fuel flue gas (ppm, dry)

$y_{H_2O,\max,oxy}$ = maximum volumetric H₂O concentration in the oxy-fuel flue gas (vol %, wet)

$\gamma_{j/k}$ = weight fraction of component j or k in the fuel (wt %, raw)

$M_{M,j/k}$ = molecular weight of component j or k (g/mol)

y_{O_2} = volume fraction of oxygen in the flue gas (vol %, dry)

NCV = net calorific value (kJ/kg)

i = index for flue gas components: H₂O, SO₂, and Hg⁰

j = index for the fuel component belonging to the respective flue gas component i : H, S, and Hg

k = index for the fuel components: W (water/moisture), S, C, and N

ad = air dried (fuel reference state)

db = dry basis (fuel reference state)

daf = dry and ash free (fuel reference state)

λ = stoichiometric ratio of combustion

$\eta_{Hg,i}$ = percentage of the Hg⁰, Hg²⁺, or Hg^{tot} capture rate (%)

$c_{Hg,i,bf}$ = mass concentration of Hg⁰, Hg²⁺, or Hg^{tot} before filter [$\mu\text{g}/\text{m}^3$ (STP)]

$c_{Hg,i,af}$ = mass concentration of Hg⁰, Hg²⁺, or Hg^{tot} after filter [$\mu\text{g}/\text{m}^3$ (STP)]

l = index indication of the Hg speciation, e.g., Hg⁰, Hg²⁺, or Hg^{tot}

MFC = mass flow controller

FGD = flue gas desulfurization

SCR = selective catalytic (NO_x) reduction

ESP = electrostatic precipitator

UBC = unburned carbon

REFERENCES

- Scheffknecht, G.; Al-Makhadmeh, L.; Schnell, U.; Maier, J. *Int. J. Greenhouse Gas Control* **2011**, *5* (1), 16–35.
- Stanger, R.; Wall, T. *Prog. Energy Combust. Sci.* **2010**, *37* (1), 69–88.
- Wall, T.; Liu, Y.; Spero, C.; Elliott, L.; Khare, S.; Rathnam, R.; Zeenathal, F.; Moghtaderi, B.; Buhre, B.; Sheng, C.; Gupta, R.; Yamada, T.; Makino, K.; Yu, J. *Chem. Eng. Res. Des.* **2009**, *87*, 1003–1016.
- Ndibe, C.; Spörl, R.; Maier, J.; Scheffknecht, G. *Fuel* **2013**, *107*, 749–756.
- Bessone, J. B. *Corros. Sci.* **2006**, *48* (12), 4243.
- Toftagaard, M. B.; Brix, J.; Jensen, P. A.; Glarborg, P.; Jensen, A. D. *Prog. Energy Combust. Sci.* **2010**, *36*, 581–625.
- Li, X.; Liu, Y.; Stanger, R.; Belo, L.; Ting, T.; Wall, T. *Gas Quality Control in Oxy-fuel Technology for Carbon Capture and Storage*; University of Newcastle: Callaghan, Australia, 2012; <http://cdn.globalccsinstitute.com/sites/default/files/publications/39971/gasqualitycontrolnoxy-opt.pdf> (accessed July 27, 2013).
- Sondreal, E. A.; Benson, S. A.; Pavlish, J. H.; Ralston, N. V. *Fuel Process. Technol.* **2004**, *85* (6–7), 425–440.
- Pavlish, J. H.; Sondreal, E. A.; Mann, M. D.; Olson, E. S.; Galbreath, K. C.; Laudal, D. L.; Benson, S. A. *Fuel Process. Technol.* **2003**, *82* (2–3), 89–165.
- Galbreath, K. C.; Zygarlicke, C. J. *Fuel Process. Technol.* **2000**, *65–66*, 289–310.
- Kolker, A.; Senior, C. L.; Quick, J. C. *Appl. Geochem.* **2006**, *21* (11), 1821–1836.
- Wilcox, J.; Rupp, E.; Ying, S. C.; Lim, D.-H.; Negreira, A. S.; Kirchofer, A.; Feng, F.; Lee, K. *Int. J. Coal Geol.* **2012**, *90–91*, 4–20.
- Senior, C. L.; Sarofim, A. F.; Zeng, T.; Helble, J. J.; Mamani-Paco, R. *Fuel Process. Technol.* **2000**, *63* (2–3), 197–213.
- Pavlish, J. H. *Fuel Process. Technol.* **2009**, *90* (11), 1327–1332.
- Sliger, R. N.; Kramlich, J. C.; Marinov, N. M. *Fuel Process. Technol.* **2000**, *65–66*, 423–438.
- Edwards, J. R.; Srivastava, R. K.; Kilgroe, J. D. *J. Air Waste Manage. Assoc.* **2001**, *51* (6), 869–877.
- Niksa, S.; Padak, B.; Krishnakumar, B.; Naik, C. V. *Energy Fuels* **2010**, *24* (2), 1020–1029.
- Dunham, G. E.; DeWall, R. A.; Senior, C. L. *Fuel Process. Technol.* **2003**, *82* (2–3), 197–213.
- Scheffknecht, G.; Farr, S.; Heidel, B.; Schwämmle, T.; Brechtel, K. *Chem. Ing. Tech.* **2012**, *84* (7), 1041–1051.
- Zheng, Y.; Jensen, A. D.; Windelin, C.; Jensen, F. *Prog. Energy Combust. Sci.* **2012**, *38* (5), 599–629.
- Pudasainee, D.; Lee, S. J.; Lee, S.-H.; Kim, J.-H.; Jang, H.-N.; Cho, S.-J.; Seo, Y.-C. *Fuel* **2010**, *89* (4), 804–809.
- Pudasainee, D.; Kim, J.-H.; Yoon, Y.-S.; Seo, Y.-C. *Fuel* **2012**, *93*, 312–318.
- Fry, A.; Cauch, B.; Silcox, G. D.; Lighty, J. S.; Senior, C. L. *Proc. Combust. Inst.* **2007**, *31* (2), 2855–2861.
- Vosteen, B. W.; Kanefke, R.; Köser, H. *VGB PowerTech* **2006**, *86* (3), 70–75.
- Galbreath, K. C.; Zygarlicke, C. J.; Tibbetts, J. E.; Schulz, R. L.; Dunham, G. E. *Fuel Process. Technol.* **2005**, *86* (4), 429–448.
- Glarborg, P.; Jensen, A. D.; Johnsson, J. E. *Prog. Energy Combust. Sci.* **2003**, *29* (2), 89–113.
- Glarborg, P. *Proc. Combust. Inst.* **2007**, *31* (1), 77–98.
- Kellie, S.; Cao, Y.; Duan, Y.; Li, L.; Chu, P.; Mehta, A.; Carty, R.; Riley, J. T.; Pan, W.-P. *Energy Fuels* **2005**, *19* (3), 800–806.
- Hocquel, M. J. T.; Unterberger, S.; Hein, K. R. G.; Bock, J. *Proceedings of the Air Quality III Conference: Mercury, Trace Elements and Particulate Matter*; Arlington, VA, Sept 10–12, 2002.
- Wang, Y.-j.; Duan, Y.-f.; Yang, L.-g.; Jiang, Y.-m.; Wu, C.-j.; Wang, Q.; Yang, X.-h. *J. Fuel Chem. Technol.* **2008**, *36* (1), 23–29.
- Hilber, T.; Thorwarth, H.; Stack-Lara, V.; Schneider, M.; Maier, J.; Scheffknecht, G. *Fuel* **2007**, *86* (12–13), 1935–1946.
- Gale, T. K.; Lani, B. W.; Offen, G. R. *Fuel Process. Technol.* **2008**, *89* (2), 139–151.
- Hower, J. C.; Senior, C. L.; Suuberg, E. M.; Hurt, R. H.; Wilcox, J. L.; Olson, E. S. *Prog. Energy Combust. Sci.* **2010**, *36* (4), 510–529.
- Senior, C. L.; Johnson, S. A. *Energy Fuels* **2005**, *19* (3), 859–863.
- Mitsui, Y.; Imada, N.; Kikkawa, H.; Katagawa, A. *Int. J. Greenhouse Gas Control* **2011**, *5*, S143–S150.
- Norton, G. A.; Yang, H.; Brown, R. C.; Laudal, D. L.; Dunham, G. E.; Erjavec, J. *Fuel* **2003**, *82* (2), 107–116.
- Serre, S. D.; Silcox, G. D. *Ind. Eng. Chem. Res.* **2000**, *39* (6), 1723–1730.
- Zhuang, Y.; Martin, C.; Pavlish, J.; Botha, F. *Fuel* **2011**, *90* (10), 2998–3006.
- Pavlish, J. H.; Hamre, L. L.; Zhuang, Y. *Fuel* **2010**, *89* (4), 838–847.
- Zheng, L.; Furimsky, E. *Fuel Process. Technol.* **2003**, *81* (1), 23–34.
- Suriyawong, A.; Gamble, M.; Lee, M.-H.; Axelbaum, R.; Biswas, P. *Energy Fuels* **2006**, *20* (6), 2357–2363.
- Hicks, W. T. *J. Chem. Phys.* **1963**, *38* (8), 1873.
- Deutsches Institut für Normung e. V. (DIN). *DIN 51900. Testing of Solid and Liquid Fuels—Determination of Gross Calorific Value by the Bomb Calorimeter and Calculation of Net Calorific Value*; DIN: Berlin, Germany, April 2000.

- (44) Deutsches Institut für Normung e. V. (DIN). *DIN 51734. Testing of Solid Mineral Fuels—Proximate Analysis and Calculation of Fixed Carbon*; DIN: Berlin, Germany, Dec 2008.
- (45) Deutsches Institut für Normung e. V. (DIN). *DIN 51718. Testing of Solid Fuels—Determination of the Water Content and the Moisture of Analysis Sample*; DIN: Berlin, Germany, June 2002.
- (46) Deutsches Institut für Normung e. V. (DIN). *DIN 51719. Testing of Solid Fuels—Solid Mineral Fuels—Determination of Ash Content*; DIN: Berlin, Germany, July 1997.
- (47) Deutsches Institut für Normung e. V. (DIN). *DIN 51720. Testing of Solid Fuels—Determination of Volatile Matter Content*; DIN: Berlin, Germany, March 2001.
- (48) Deutsches Institut für Normung e. V. (DIN). *DIN 51732. Testing of Solid Mineral Fuels—Determination of Total Carbon, Hydrogen and Nitrogen—Instrumental Methods*; DIN: Berlin, Germany, Aug 2007.
- (49) Deutsches Institut für Normung e. V. (DIN). *DIN 51724. Testing of Solid Fuels—Determination of Sulfur Content*; DIN: Berlin, Germany, July 2012.
- (50) Deutsches Institut für Normung e. V. (DIN). *DIN 51733. Testing of Solid Mineral Fuels—Ultimate Analysis and Calculation of Oxygen Content*; DIN: Berlin, Germany, Dec 2008.
- (51) Deutsches Institut für Normung e. V. (DIN). *DIN 51727. Testing of Solid Fuels—Determination of Chlorine Content*; DIN: Berlin, Germany, Nov 2011.
- (52) Deutsches Institut für Normung e. V. (DIN). *DIN 22022. Solid Fuels—Determination of Contents of Trace Elements*; DIN: Berlin, Germany, July 2013.
- (53) Deutsches Institut für Normung e. V. (DIN). *DIN 51729-11. Testing of Solid Fuels—Determination of Chemical Composition of Fuel Ash—Part 11: Determination by Inductively Coupled Plasma Emission Spectrometry (ICP—OES)*; DIN: Berlin, Germany, Nov 1998.
- (54) Verein Deutscher Ingenieure (VDI). *VDI 2462, Blatt 2. Measurement of Gaseous Emissions—Determination of Sulphur Trioxide in Water Vapour Containing Exhaust Gas—Condensation Method*; VDI: Düsseldorf, Germany, Nov 2011.
- (55) Deutsches Institut für Normung e. V. (DIN). *DIN EN 1911. Stationary Source Emissions—Determination of Mass Concentration of Gaseous Chlorides Expressed as HCl—Standard Reference Method; German Version EN 1911:2010*; DIN: Berlin, Germany, Dec 2010.
- (56) Deutsches Institut für Normung e. V. (DIN). *DIN EN ISO 10304-1. Water Quality—Determination of Dissolved Anions by Liquid Chromatography of Ions—Part 1: Determination of Bromide, Chloride, Fluoride, Nitrate, Nitrite, Phosphate and Sulfate (ISO 10304-1:2007)*; German Version EN ISO 10304-1:2009; DIN: Berlin, Germany, July 2009.
- (57) Zhuang, Y.; Pavlish, J. H.; Lentz, N. B.; Hamre, L. L. *Int. J. Greenhouse Gas Control* **2011**, 5, 136–S142.
- (58) SEMTECH AB. *TÜV-Report 936/809007/B: Bericht über die Eignungsprüfung der Messeinrichtung HG 2010 für Quecksilber und seine Verbindungen der Firma*; SEMTECH AB: Lund, Sweden, 2000.
- (59) Hocquel M. Ph.D. Thesis, Universität Stuttgart, VDI Fortschritt-Berichte, Reihe 15, Number 251, 2004.
- (60) Laudal, D. L.; Thompson, J. S.; Pavlish, J. H.; Brickett, L. A.; Chu, P. *Fuel Process. Technol.* **2004**, 85 (6–7), 501–511.
- (61) Metzger, M.; Braun, H. *Chemosphere* **1987**, 16 (4), 821–832.
- (62) Deutsches Institut für Normung e. V. (DIN). *DIN 1343. Reference Conditions, Normal Conditions, Normal Volume; Concepts and Values*; DIN: Berlin, Germany, Jan 1990.
- (63) Deutsches Institut für Normung e. V. (DIN). *DIN 22022-6. Testing of Solid Fuels—Determination of Trace Elements—Part 6: Evaluation and Declaration of Results*; DIN: Berlin, Germany, Dec 2001.
- (64) Jäger, U.; Thorwarth, H.; Acuna-Caro, C.; Scheffknecht, G. *Verhalten von Quecksilber und seinen Verbindungen in staubhaltigen Rauchgasen*; IVD-Berichte: Stuttgart, Germany, 2006; AiF Research Project 13534N.
- (65) Thorwarth, H.; Stack-Lara, V.; Unterberger, S.; Scheffknecht, G. *Proceedings of the Air Quality V Conference: Mercury, Trace Elements, SO₃ and Particulate Matter*; Arlington, VA, Sept 19–21, 2005.